Evaluating the accuracy of two satellite-based Quantitative Precipitation Estimation products and their application for meteorological drought monitoring over the Lake Victoria Basin, East Africa

Priyanko Das, Zhenke Zhang & Hang Ren

Taylor & Francis
Taylor & Francis Group

Evaluating the accuracy of two satellite-based Quantitative Precipitation Estimation products and their application for meteorological drought monitoring over the Lake Victoria Basin, East Africa

Priyanko Das[a,b], Zhenke Zhang[a,b] and Hang Ren[c]

[a]Center of African Studies, Nanjing University, Nanjing, China and School of Geographic and Oceanographic Sciences, Nanjing University, Nanjing, China; [b]Center of African Studies, Nanjing University, Nanjing, China and School of Geographic and Oceanographic Sciences, Nanjing University Nanjing China; [c]Institute of Population Studies, Nanjing University of Posts and Telecommunications, Nanjing, Jiangsu province, China

ABSTRACT

This study evaluates the high-resolution satellite estimated long-term precipitation data for monitoring the drought condition over the Lake Victoria Basin (LVB) from 1984 to 2020. Standardized Precipitation Indices (SPI) were used to capture the short, medium and long-term meteorological drought conditions at multiple time scales (i.e. 3, 6, and 12). For these, the following two primaries Quantitative Precipitation Estimation (QPEs) products were employed – 1) Climate Hazards group Infra-Red Precipitation with Station (CHIRPS), and 2) the Precipitation Estimation from Remotely Sensed Information using Artificial Neural Network -Climate Data Record (PERSIANN-CDR). This dataset was compared based on the observation data obtained from the Climate Research Unit (CRU) over the nine selected regions surrounding lake basins. The performance of these two QPEs products was evaluated using seven statistical metrics. The findings of this study indicate that the CHIRPS and PERSIANN-CDR datasets could capture the behavior of drought magnitude based on the time scale of SPI-3, SPI-6, SPI-12. The results indicate that 2012 and 2017 are significant severe drought years in the recent decade over LVB. However, the CHIRPS datasets provide good agreement (Correlation Coefficient (CC) = 0.65) with observation, whereas PERSIANN-CDR present satisfactory results (CC = 0.54). In addition, Hurst (H) exponent was used to predict the future drought trend and found that the CHIRPS performed well to predict the degree of drought trend. Therefore, this study considers the CHIRPS product for near-real-time drought monitoring and PERSIANN-CDR for historical drought assessment. Moreover, the outcome from the H values is greater than 0.5, which indicates the future drought trend would be decreased over LVB. These results are useful for developing the strategies for drought hazards and water resource management in LVB.

1. Introduction

Drought is recognized as a costly natural disaster worldwide that threatens water, food resources, agriculture, and environmental health (Mohseni et al. 2021). Monitoring and forecasting the drought events are used to assess the impact of extreme weather events on the respective population (Bouaziz, Medhioub, and Csaplovisc 2021). Under climate change, drought conditions affect water level, natural ecosystem, agriculture production, and shortage in the food supply from the last decade (Guo et al. 2016). Various studies suggest that the wetter region would receive more devastating drought conditions in the future (Yaseen et al. 2021). Increased global air temperature and evapotranspiration contribute to a warm climate, creating severe drought (Musonda et al. 2020). In this present situation, society finds a more sustainable and nature-based solution to tackle drought conditions (Dikici 2020; Huang and Wang 2020; Trinder and Liu 2020; Shao et al. 2021). Therefore, drought monitoring and forecasting are

essential for risk management and established innovative strategies for drought mitigation (Dehghan et al. 2020). Classification of drought is categorized into four types – 1) Meteorological, 2) agricultural, 3) hydrological, and 4) socio-economic drought, which is measured using different approaches (Malik et al. 2021; Mohseni et al. 2021).

Meteorological drought is one of the primary drought types due to adverse precipitation conditions from the average and extended time (Pathak and Dodamani 2020). Although, the frequency of the meteorological drought does not depend on the average precipitation (Yaseen et al. 2021). Various types of meteorological drought indices such as Standard Precipitation Index (SPI) (Kubicz 2018; Pathak and Dodamani 2020; Liu et al. 2021), Precipitation Normal Index (PNI) (Salehnia et al. 2017; Abrha and Hagos 2019), Deciles Index (DI) (Salehnia et al. 2017; Dikici 2020; Yaseen et al. 2021), Rainfall Anomaly Index (RAI) (Abrha and Hagos 2019), developed and used to monitor drought condition at regional or global

scale (Guo et al. 2016). However, various studies found that the maximum drought occurs due to the decline of precipitation in a region, and meteorological drought indices are mainly used to describe this condition (Kassaye et al. 2021). In addition, the Standardized Precipitation Index (SPI) and the Standardized Precipitation Evapotranspiration Index (SPEI) are the most commonly used drought indices (Kubicz 2018; Dikici 2020). Although, in 2009 World Meteorological Organization (WMO) recommended the SPI as an essential meteorological drought index (WMO 2012). Hayes et al. (2011) found that the SPI is a standard index to describe the regional drought indices used worldwide. Therefore, this study used the SPI index to track the meteorological drought condition over the Lake Victoria Basin (LVB).

Precipitation is an important variable for estimating the meteorological drought indices (Zhong et al. 2019). It is challenging to get station-based meteorological data, and most of the time is unavailable. Satellite remote sensing instruments and different precipitation retrieved algorithms provide Quantitative Precipitation Estimation (QPEs) datasets and are available for public use. The QPEs algorithm is developed with a combination of Passive Microwave (PMW) and Infrared (IR) sensors such as Tropical Measuring Mission (TRMM) Multi-satellite Precipitation Analysis (TMPA) (Atiah et al. 2020; Shobeiri, Sharafati, and Neshat 2021), Integrated Multi-Satellite Retrievals for Global precipitation measurement (IMERG) (Zhang et al. 2021), the Climate Prediction Center morphing technique (CMORPH) (Zhao and Ma 2019). However, the application of these QPEs products for drought monitoring is restricted due to their short observation period (shorter than 20 years) (Zhong et al. 2019). In general, drought index calculation usually requires at least 30 years of data records (McKee, Doesken, and Kleist 1993.; Zhao and Ma 2019). Although, WMO suggests that the long term (more than 30 years) historical precipitation record is reliable for SPI calculation (Guo et al. 2016). For this reason, some long term QPEs were developed, such as Precipitation Estimation from Remotely Sensed Information using Artificial Neural Network Climate Data Record (PERSIANN-CDR) (Guo et al. 2016; Mohseni et al. 2021), Climate Hazards Group InfraRed Precipitation with Station data (CHIRPS) (Bouaziz, Medhioub, and Csaplovisc 2021). These products are suitable for drought monitoring due to their long-term data record (more than 30 years) (Lai et al. 2019; Zhong et al. 2019).

Previous studies suggest that the QPEs of CHIRPS and PERSIANN-CDR perform well for drought monitoring on a global and regional scale (Gao et al. 2018; Salmani-Dehaghi and Samani 2019; Zhao

and Ma 2019; Chen et al. 2020). Furthermore, these two QPEs products have been widely used during various hydrological simulations (Arheimer 2021; Shahid et al. 2021) and meteorological applications such as drought forecasting (Danandeh Mehr et al. 2020; Dehghan et al. 2020; Pandey et al. 2020). Lai et al. (2019) monitor hydrological drought conditions using long-term QPEs (PERSIANN-CDR, CHIRPS) products. The studies found that both QPEs products are reliable and effective for drought calculation. However, drought monitoring and forecasting using PERSIANN-CDR showed good agreement of probabilistic distribution with in-situ data (Shrestha et al. 2017). de Brito et al. (2021) used PERSIANN-CDR and CHIRPS products for meteorological drought monitoring, and a summary of this study showed that the PERSIANN-CDR performed better than CHIRPS. In addition, Santos et al. (2021) found that the PERSIANN-CDR rainfall products have a strong ability for capturing the SPI and Drought Severity (DS) classification.

Climate change influenced the rainfall pattern in the Great Lakes of Africa and affected 30 million people (Awange et al. 2013). In the LVB, rainfall patterns are defined by a bimodal cycle that is regulated by the north-south migration of the Intertropical Convergence Zone (ITCZ) (Kizza et al. 2009). Overall rainfall trends from the past decades indicate the drier climate over LVB caused the drought condition. Previous studies identify some drought years based on the annual rainfall anomaly, such as 1992 highlighted (Awange 2021). However, these two QPEs products (CHIRPS and PERSIANN-CDR) have not yet been tested for drought monitoring in the semiarid region of LVB (Awange 2021). Also, this topic is interesting for watershed managers and policymakers of this region. Thus, the main objective of this study is to evaluate the efficiency of CHIRPS and PERSIANN-CDR product to estimate the drought event and future drought trend in LVB.

The current study is devoted to evaluating and comparing two widely used QPEs satellite products at a regional scale to estimate and forecast the drought event at LVB to assist the water resource managers in improving the policy and management. The specific objective of this study is 1) to evaluate two QPEs products (CHIRPS and PERSIANN-CDR) for meteorological drought monitoring at the regional scale, 2) to evaluate the meteorological drought assessment using the SPI index in an East African drought-prone region (Lake Victoria Basin) for 37 years (1984–2020), and 3) to predict the spatial pattern of drought events in future using Hurst exponent. Although, this QPEs product has not yet been used to investigate the drought events and predict the degree of drought in LVB, which is valuable and interesting for water resource management of this region.

2. Materials and methods

2.1. Lake Victoria Basin

Lake Victoria Basin is the world's second-largest freshwater reservoir (Figure 1), which directly contributes to 30 million people and indirectly supports 340 million people along the Nile basin (Awange et al. 2013). The surface area of Lake Victoria is roughly 68,800 km², and the catchment area covers 194,000 km². This basin shared the surface area within the three countries of East Africa- Kenya, Uganda, and Tanzania (Kizza et al. 2012). Also, it is one of the major agricultural production areas and breadbasket in this region (Anyah, Semazzi, and Xie 2006). Thus, the Lake is essential for the East African region's energy supply, fisheries, domestic and industrial water supply. In the LVB, 80% of the water balance is dominated by evaporation, rainfall and the rest of the 20% of water received inflow water from 17 tributaries (Odada et al. 2003). However, the basin also plays a significant role in biodiversity conservation and tourism activities. Although, Major vegetation types across the LVB include cropland, woodland, grassland, savannas, and climatic patterns (Mugo et al. 2020).

Wet or dry conditions characterize the climate variability of LVB. This condition is based on the Sea Surface Temperature (SST) of the equatorial Indian ocean (Anyah, Semazzi, and Xie 2006). The basin received 120–160 mm annual mean rainfall with bimodal seasonal distribution (Phoon, Shamseldin,

and Vairavamoorthy 2004). The peak of this rainfall occurs during March-May and November-December with a unique diurnal system. Also, significant rainfall is received from the humid Congo air mass over the western and northwestern parts (Awange et al. 2013). As a result, the average surface temperature of LVB 25.4°C is 3.5°C higher than the surrounding station air temperature (Yin and Nicholson 1998). It is projected to increase 3–4°C by the end of this century (Awange et al. 2013).

2.2. Datasets

2.2.1 Observation-based Grided rainfall datasets

The distribution of rain-gauge stations in LVB is contributed by East Africa's five countries (Uganda, Kenya, Tanzania, Rwanda, Burundi). Therefore, it is quite difficult to obtain rain-gauge datasets from all the meteorological stations. Also, most stations have 70% missing data, which could not be considered for long term drought monitoring and evaluating the QPEs precipitation datasets. This study obtained observation datasets from the Climate Research Unit Gridded Time Series (CRU TS) as reference data to evaluate meteorological drought indices utility of the QPEs. This high-resolution (0.5°) gridded product provides station-based monthly datasets with no missing values (Harris et al. 2020). The datasets include various climate variables such as precipitation, mean temperature, Potential Evapotranspiration (PET), cloud cover,
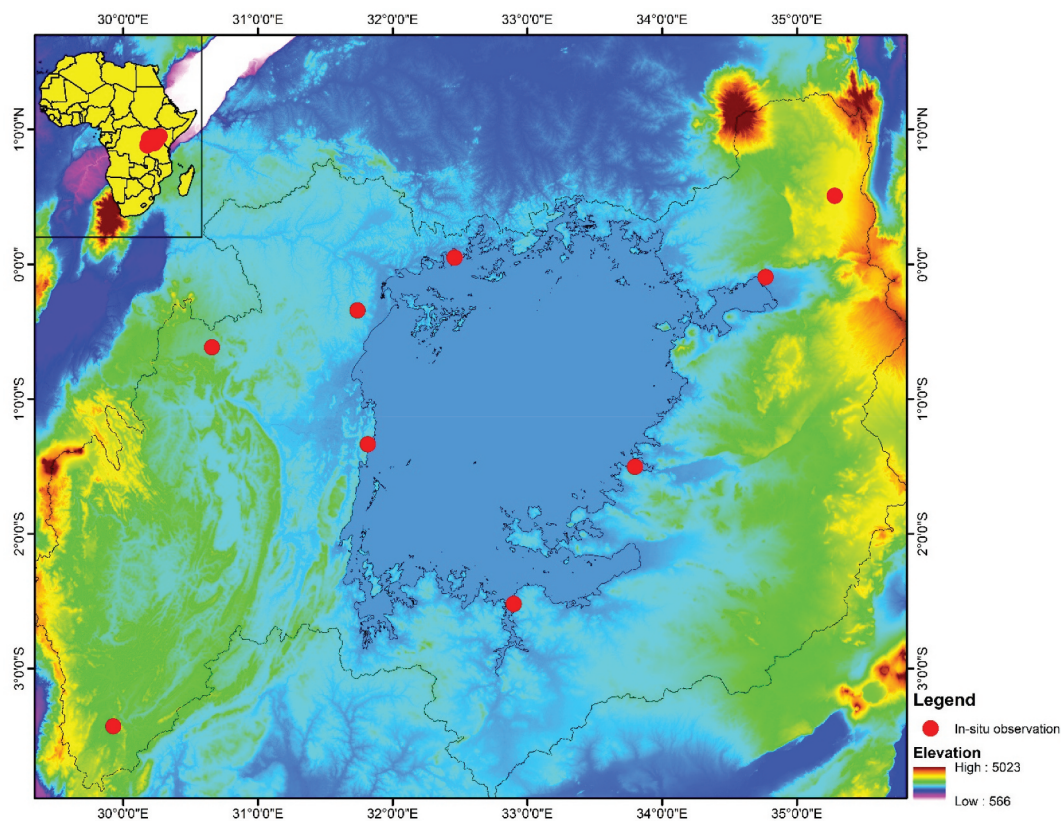

Figure 1. Location of the Lake Victoria Basin (LVB), East Africa, and CRU observation with altitude.

maximum and minimum temperature, vapor pressure, etc. (Mutti et al. 2020). The CRU TS data have been produced from an extensive weather station network using the Angular-Distance-Weighting (ADW) interpolation method. The precipitation observation using ADW provides improved traceability in each grid and maintain quality control due to the high density of station gauge (van der Schrier et al. 2013). Many rain gauge stations are used to generate Grided CRU TS datasets and have undergone strict quality control and homogeneity check (Harris et al. 2020). Although, most of the previous studies used CRU-TS data as observation data to calculate SPI for drought monitoring. Zhao and Ma (2019) utilize CRU TS data as reference data to evaluate the four QPEs products for drought monitoring at the global scale. Mutti et al. (2020) compared the gridded CRU TS data to observation for water balance monitoring and found a strong correlation ($r = 0.87$) over the semi-arid region for long term precipitation data. However, many studies used grided observation data as reference datasets to evaluate the QPEs product for drought monitoring (Ionita, Scholz, and Chelcea 2016; Guo et al. 2016; Zhong et al. 2019). Therefore, with the high density of the gauge network and the high precipitation quality, the CRU TS is reliable and suitable for drought monitoring and reference to evaluate the QPEs. This study retrieved CRU TS monthly data from the Climate Research Unit (CRU) website (https://sites.uea.ac.uk/cru/data) from 1984 to 2020.

2.2.2 CHIRPS

The Climate Hazard Group (CHG) at the United States Geological Survey (USGS) and the University of California laboratory developed the CHIRPS datasets (Gao et al. 2018). The datasets used satellite imagery with observational data and Climate Hazards Group Precipitation Climatology (CHPclim) (Zhong et al. 2019; Shahid et al. 2021). This data provides long-term precipitation with 0.05° spatial resolution and covers most of the earth surface (50° N to 50° S). The generation of CHIRPS product use three-component, where the first component is based on monthly rainfall data with 0.05° resolution, the second component includes Climate Hazard's group precipitation which uses infrared precipitation, and the last component is interpolated the observed data from various sources (de Brito et al. 2021; Ghozat, Sharafati, and Hosseini 2021). Therefore, this dataset is suitable for long-term drought monitoring and forecasting. This study collected the latest version of CHIRPS data from https://www.chc.ucsb.edu/data/chirps website during 1984–2020 and used it for QPEs evaluation. However, very few stations were used to generate CHIRPS products over East Africa, and those stations were not considered for avoiding the biasing results.

2.2.3 PERSIANN-CDR

The Center for Hydrometeorology and Remote Sensing (CHRS) at the University of California developed the Precipitation Estimation from Remotely Sensed Information Using Artificial Neural Networks (PERSIANN) data and later integrated it with the National Climate Data Center's (NCDC) Climate Data Record (CDR) as a new product PERSIANN-CDR (Guo et al. 2016; Nguyen et al. 2019). These are the first satellite precipitation estimation system that used a machine learning technique known as Artificial Neural Network (ANN). Monthly infrared images from the grided satellite (GridSat-B1) combined with monthly Global Precipitation Climatology Project (GPCP) data (Nguyen et al. 2019). The PERSIANN-CDR provides daily rainfall products with spatial resolution 0.25° and Global coverage from 60° N to 60° S (Atiah et al. 2020). This dataset is useful for long-term climate change studies, hydrological modeling, and drought prediction. Therefore, the study retrieved PERSIANN-CDR data from the CHRS website (https://chrsdata.eng.uci.edu/) during 1984–2020 for evaluation QPEs.

2.3. Standardized precipitation index

SPI (McKee, Doesken, and Kleist 1993) is a widely used statistical drought indicator based on the probability of precipitation anomaly (Zhong et al. 2019). Only precipitation data was required for SPI, which is the main reason for its applicability for various meteorological drought-related applications (Tigkas, Vangelis, and Tsakiris 2019). This method defines the severity of dry and wet conditions based on precipitation records to a probabilistic distribution (i.e. Gamma distribution, Pearson III) (de Brito et al. 2021), and standardization of these values adjust to a normal distribution (Santos et al. 2021). Therefore, the time series of cumulative precipitation applied multiple times (i.e. 3, 6, 9, 12, 24, 48 months) and gamma distribution function fitted to a given precipitation frequency (Liu et al. 2021). Although, more details regarding the estimation of SPI can be found in Gao et al. (2018), Mohseni et al. (2021) and Liu et al. (2021).

This study estimates the SPI at multiple scales (SPI-3, SPI-6, and SPI-12) for monitoring the short, medium, and long-term meteorological drought conditions over LVB from 1984 to 2020. These meteorological drought indices were performed based on the QPEs precipitation and CRU observation datasets from 1984 to 2020. Precipitation data were adjusted for SPI using a probabilistic distribution function for two parameters, β and α. However, 81 (9-time series × 3 datasets × 3-time scale) time series with 444 (37×12) SPI values were evaluated in various

**Table 1.** Drought severity categories based on SPI (Mckee et al., 1993).

Sl.No.	Drought Categories	SPI
1	Extremely wet	>2.0
2	severe wet	1.5 to 1.9
3	Moderately wet	1 to 1.49
4	Near Normal	0.99 to −0.99
5	Moderately dry	−1 to −1.49
6	severe dry	−1.5 to −1.9
7	Extremely dry	<-2.00

categories. Also, dry and wet events were assessed based on the various categories of SPI index values shown in Table 1.

2.4. Evaluation method and statistical metrics

This study compared the meteorological drought pattern at temporal and spatial scales (Figure 2). Although, two methods are widely used to compare the satellite and observation-based precipitation data. Most researchers estimate the spatial rainfall using interpolation approaches such as Inverse Distance Weighted (IDW) and Kriging (Gao et al. 2018) from the rain gauge and compare with satellite products using pixel to pixel comparison. Some researchers extracted precipitation data where the rain gauge located in the study region, then compared it with different products (Mutti et al. 2020). The second approach used the arithmetic average of four to nine pixels surrounding the rain gauge (Shrestha et al. 2017). de Brito et al. (2021) used 38 grid cells of PERSIANN-CDR and CHIRPS precipitation data associated with 38 rain gauge stations and performed interpolation using the spatial pixel averaging method with a grid resolution of 0.250. In this study, fine-resolution satellite data (0.5° × 0.5°) represent the areal average of precipitation within the pixel where the rain gauge is located. In general, evaluating the monthly rainfall time series from nine CRU observations was selected from the nine-rain gauge station. These observational data were compared to the QPEs products, and the precipitation data (CHIRPS and PERSIANN-CDR) were extracted using the pixel averaging method. Although, a bilinear interpolation
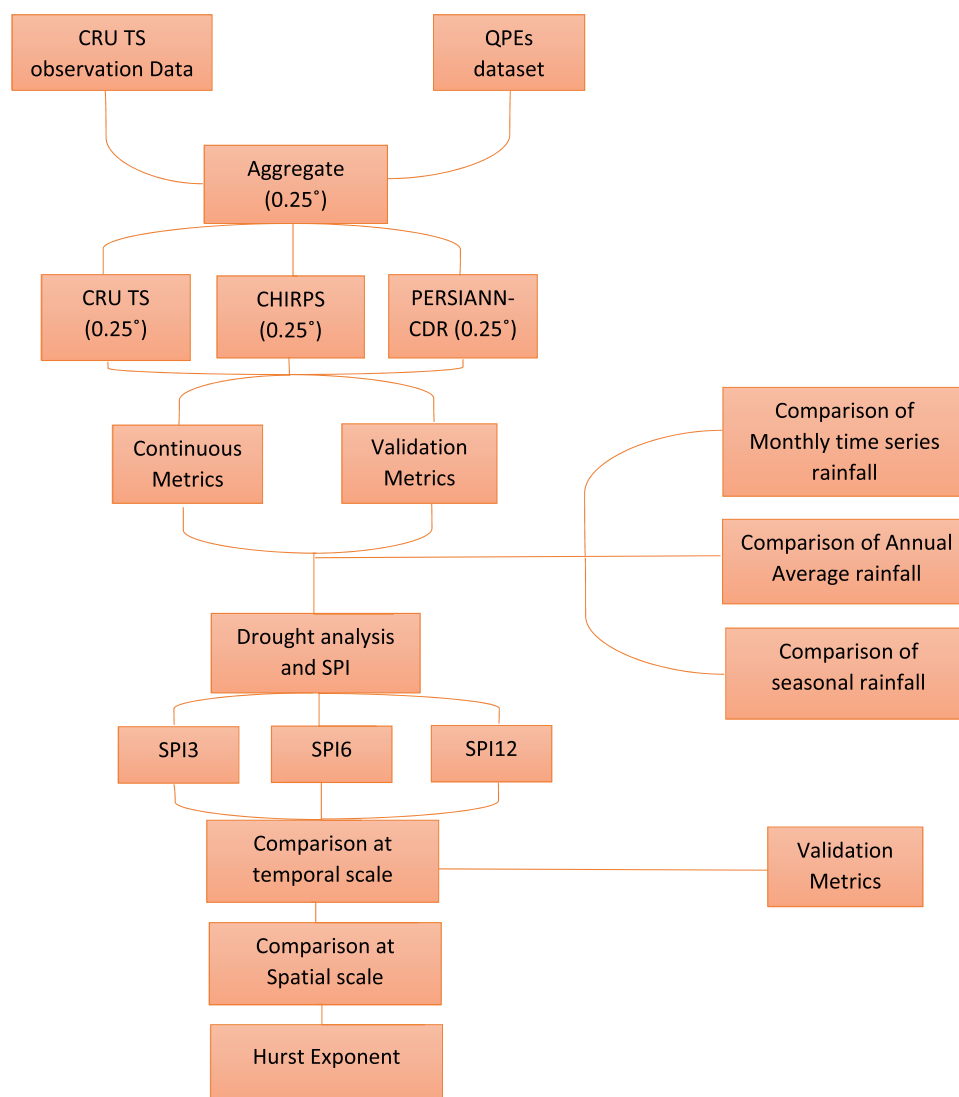
Figure 2. Flowchart diagram of the proposed method.

method was performed to resampled QPEs product into a 0.25° spatial grid. This data was arranged on a monthly series to calculate the SPI at multiple scales.

The spatial distribution of the three continuous metrics (PBIAS, MKGE score, Theil'U) was used to evaluate the performance of CHIRPS and PERSIANN-CDR precipitation products against CRU observational data (Table 2). These metrics were used to compare the precipitation product with CRU observation on a pixel scale on different parts of the study region. The Percentage of BIAS (PBIAS) estimates the over/under-estimation of precipitation product, where positive value considers overestimation and negative value represent underestimation (Shrestha et al. 2017). The performance of QPEs products was assessed using Modified Kling-Gupta Efficiency (MKGE) score (Kling, Fuchs, and Paulin 2012), which includes the liner correlation (r), bias ratio (β) and variability ratio (γ), followed by the Zhu et al. (2021). Also, Theil'U is used to predict the accuracy of forecasting values, whereas close to 0 indicates perfect forecasting and closes to 1, showing some error in the products (Rahman et al. 2019, 2020).

In addition, four commonly used statistical validation metrics were selected to evaluate the performance of satellite-based precipitation datasets from 1984 to 2020, shown in Figure 3. First, the Correlation Coefficient (CC) quantifies the strength of a linear relationship between two variables. Second, the Mean Bias Error (MBE) described the systematic error of the estimated data. In addition, Mean Absolute Error (MAE) was employed to present the magnitude of error from drought indices. Finally, the Root Mean Square Error (RMSE) compares the differences between CRU observation and QPEs estimated drought indices (Saeedi, Sharafati, and Tavakol 2021). The CC, MBE, MAE, and RMSE were also selected to investigate the detection of drought events in LVB quantitatively. Table 2 shows the statistical metrics used to validate QPEs precipitation product and CRU observation, where "P" is the QPEs

precipitation, "O" is CRU observed precipitation, μ and σ Represent the mean value and the standard variation, n is a no. of sample size.

2.5. Hurst exponent

The Hurst (H) exponent is first introduced by Hurst (1951) to understand the long term memory behavior of a variable in a time series at the Nile River, Egypt (Noorisameleh, Gough, and Mirza 2021). This method is very useful for understanding a time series characteristics without making assumptions of statistical restriction (Tatli 2015). There are numerous ways to estimate the Hurst exponent used by various literature (Feng et al. 2020; Millán, Macías, and Rabelo-Lima 2021; Shahid and Rahman 2021; Wei et al. 2021). Among them, the rescaled-range (R/S) analysis is the best-known method to calculate the H exponent and was suggested by Mandelbrot and Wallis (1969). The primary idea behind R/S analysis is to examine the statistical characteristics of a changing time scale of a given series (Huang et al. 2016). Therefore, we estimate the R/S based H exponent for this study to understand the future drought trend. Although, more details about the step-by-step procedure for calculating the R/S based H exponent can be found in Oliver and Ballester (1996). In general, the estimated H exponent value ranges from 0 to 1 based on the SPI time series. When H = 0.5, it means that the time series has no changes. Whereas 0.5 < H < 1 indicates the time series has continuous properties, and the future trend of SPI is consistent with the past trend. In addition, 0 < H < 0.5 indicates the SPI time series is anti-continuous, the future trend is opposite to the past.

3. Results

3.1. Evaluation of precipitation datasets

The analysis of QPEs is considered rainfall data from nine LVB regions obtained from CRU observation with 37 years of long data record and utilized to monitor the meteorological drought indices. It should be noted that various studies attempted to investigate the performance of the QPEs products over the different climatic regions (Gao et al. 2018; Lai et al. 2019; Chen et al. 2020; de Brito et al. 2021). But the accuracy of QPEs products depends on the area properties and its local climate (Mohseni et al. 2021).

The average annual rainfall over the LVB was 160 mm, with monthly values 250 mm for wet season (MAM and OND) and 80 mm for dry months (JJAS). Therefore, the June, July, August, and September (JJAS) months are the lowest rainfall recorded dry months. This section presents the monthly time series of QPEs and CRU observation

Table 2. Calculation of the statistical metrics to validate the QPEs and CRU observation products.

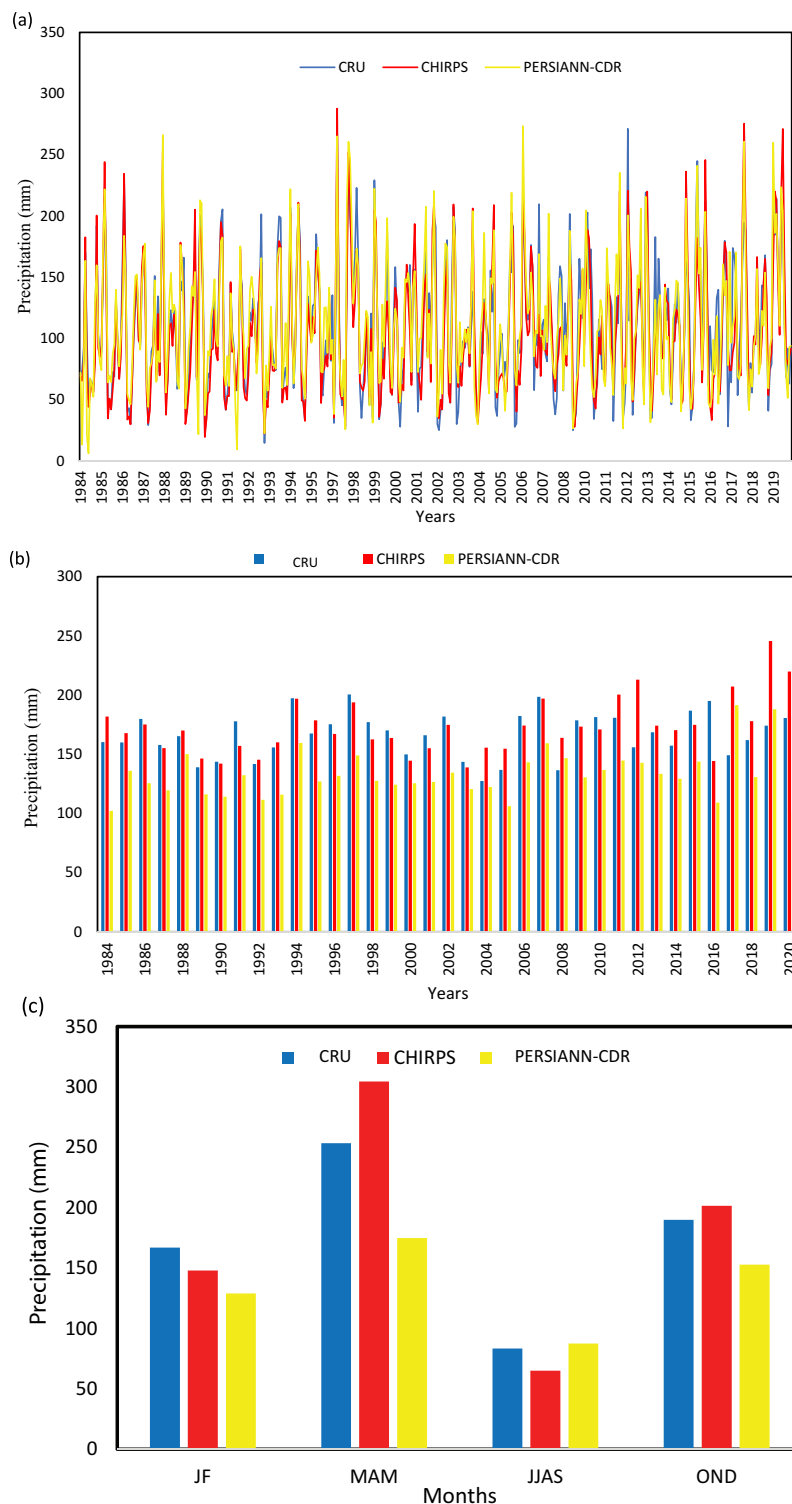| Statistical Metrics	Equation
PBIAS	$PBIAS = \frac{\sum(O_i - P_i)}{\sum O_i} X100$
MKGE Score	$MKGE = 1 - \sqrt{(CC-1)^2 + \left(\frac{\mu(P)}{\mu(O)} - 1\right)^2 + \left(\frac{\sigma(P)/\mu(P)}{\sigma(O)/\mu(O)} - 1\right)^2}$
Theil's U	$U = \sqrt{\frac{1}{n}\sum_{i=1}^{n}(P_i - O_i)^2 / \sum_{i=1}^{n} P_i^2}$
CC	$r = \frac{\sum_{i=1}^{n}(O_i - \bar{O})(P_i - \bar{P})}{\sqrt{\sum_{i=1}^{n}(O_i - \bar{O})^2}\sqrt{\sum_{i=1}^{n}(P_i - \bar{P})^2}}$
MBE	$MBE = \frac{1}{n}\sum_{i=1}^{n}(P_i - O_i)$
MAE	$MAE = \frac{1}{n}\sum|P_i - O_i|$
RMSE	$RMSE = \sqrt{\frac{1}{n}\sum(P_i - O_i)}$

Figure 3. (a) Time Series of Monthly mean precipitation(b) Annual mean difference(c) Seasonal variation between QPEsprecipitation product and CRU observation

precipitation in Figure 3(a). Although, a similar pattern was recognized between all the QPEs product and In-situ datasets. The CHIRPS showed the overestimated precipitation compared to CRU observation for the wet season (MAM and OND), whereas PERSIANN-CDR indicates underestimation precipitation. Figure 3(b) shows the average annual rainfall between QPEs and CRU observation. This annual average rainfall showed the same rainfall pattern between CHIRPS and CRU observation (Figure 3(b)). However, in recent years, the CHIRPS showed some overestimated rainfall records (nearly 40 mm) than CRU observation data (2011, 2012, 2014, 2017, 2018, 2019, and 2020), whereas PERSIANN-CDR shows underestimating rainfall. CHIRPS data shows overestimation
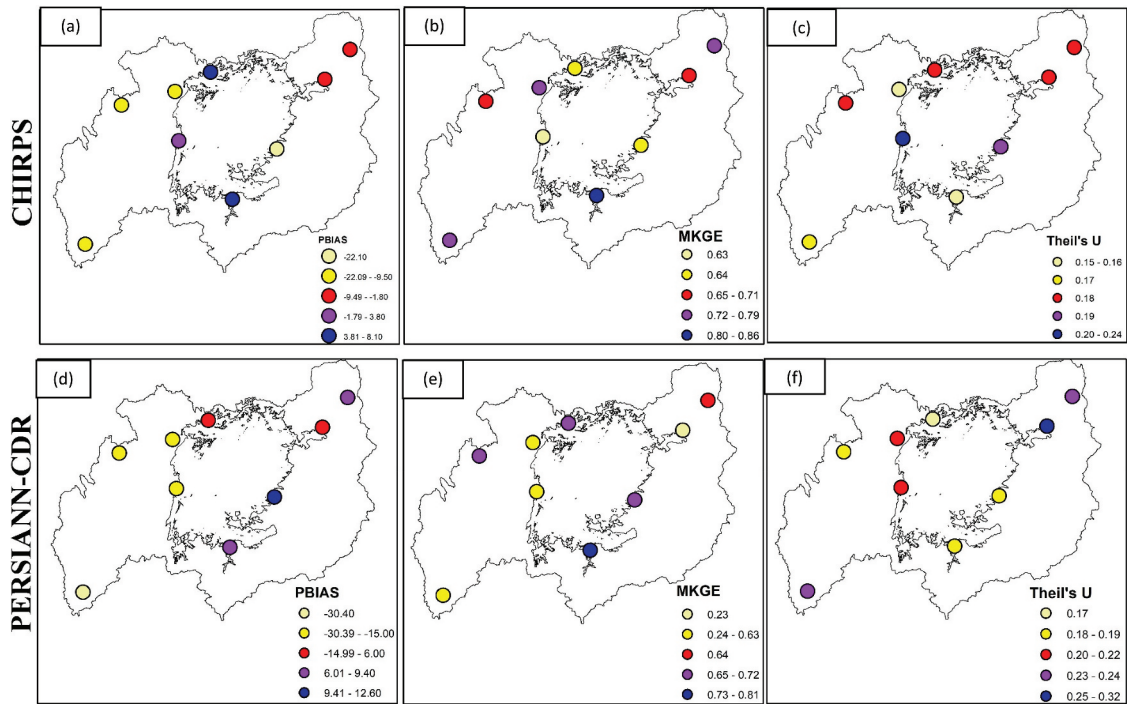
Figure 4. Spatial distribution of Continuous Metrics of PBIAS (a,d), MKGE score (b,e), Theil'U (c,f) for QPEs estimated Precipitation data compare to CRU observation.

in wet seasons and underestimate in the dry seasons (Figure 4(c)). Also, PERSINN-CDR shows underestimated rainfall during the two wet seasons (MAM and OND) and one dry season (JJAS).

The statistical analysis between CRU observation and QPEs precipitation was carried out for individual grids over the LVB. The various statistical matrices plot between In-situ and QPEs showed in Figure 4 and Figure 5. The spatial performance of continuous metrics over nine regions in LVB was shown in Figure 4 using the Kriging interpolation method. The qualitative ratings of PBIAS indicate that most areas have 'very good performance for CHIRPS and PERSIANN-CDR products (Table 3). In the eastern part of the LVB, the performance rating is "good" for CHIRPS. Also, the southwestern corner of the studied region shows a "good" rating for PERSIANN-CDR compared to the CRU observation (Figure 4(a, d)).
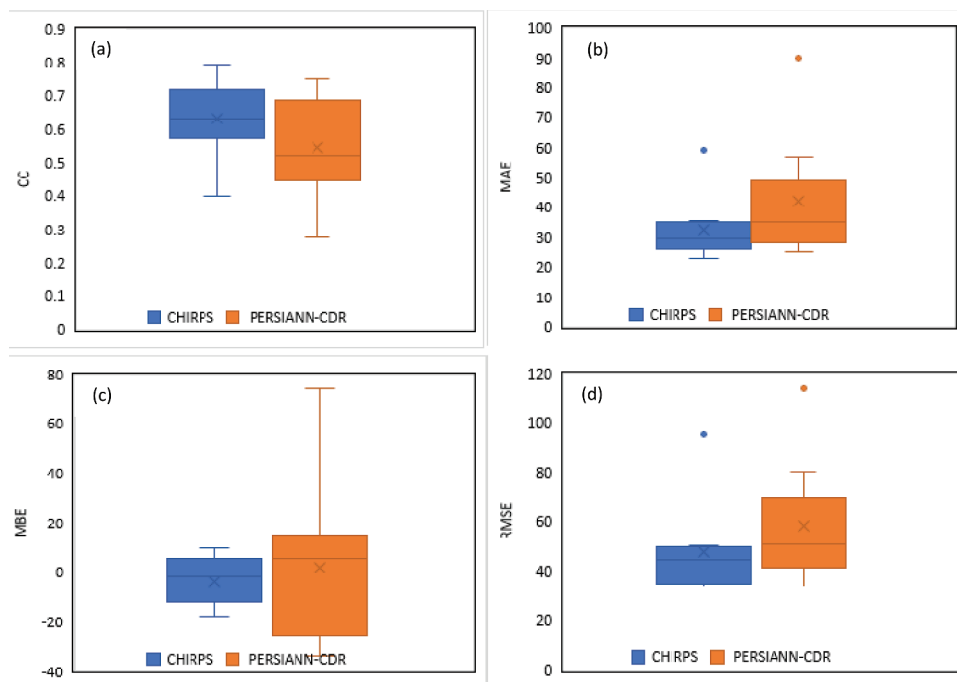

Figure 5. Validation metrics of CC (a), MBE (b), MAE(c), and RMSE (d) for QPEs estimated precipitation data compare to CRUobservation on the monthly scale.

Table 3. Range of adopted values of the PBIAS for a particular qualitative rating (Shrestha et al., 2017).

Performance rating	PBIAS (%)
Very good	<±15
Good	±15 – ±30
Satisfactory	±30 – ±55
Unsatisfactory	±55

The qualitative ratings for all the regions have varied from "very good" to "good", and there is no unsatisfactory rating found within this region. The MKGE score for QPEs products compared to the CRU observation. The smaller MKGE score was found in the northeast part of the studied region for the PERSIANN-CDR product, indicating poor performance with the lowest value of (0.23) (Figure 4(e)). The highest MKGE score was found for the CHIRPS products, which varied from 0.63 to 0.83 and indicated excellent performance (Figure 4(b)). The distribution of Theil'U indicates that the CHIRPS and PERSIANN-CDR product accurately detect the precipitation event against CRU observation (Figure 4(c, f)). Although, most of the regions represent better forecasting with smaller values (closed to 0). However, the CHIRPS product has better accuracy in detecting the precipitation event compared to PERSIANN-CDR.

The correlation coefficient correlation indicates that the CHIRPS data performed better than PERSIANN-CDR data at annual and monthly scales. Figure 5(a) showed that the relationship between CRU observation and CHIRPS estimated data (0.803) was higher than CRU and PERSIANN-CDR estimated data (0.734). CHIRPS estimated data shown (Figure 5(b)) the lower MAE value (16.97 mm) compared to PERSIANN-CDR estimated data (20.67 mm) at annual and monthly scale. The MBE for CHIRPS and PERSIANN-CDR estimated data has an average value of −3.65 and 2.08, respectively shown in Figure 5(c).

Moreover, the RMSE values (Figure 5(d)) were lower for CHIRPS estimated data (23.69 mm) which consider the monthly mean precipitation based on the CRU measurement (300 mm). It should be noted that both QPE's satellite products' overall performance can be considered suitable for meteorological drought monitoring and other allied studies. However, the statistical comparison shows the better CC and lowest error in terms of MAE, RMSE, and MBE for CHIRPS data in almost all the points, indicating that the CHIRPS data performed better in comparison of PERSIANN-CDR.

3.2. Drought monitoring and SPI

3.2.1. Comparison of SPI based drought events at the temporal scale

The SPI-3, SPI-6, and SPI-12 indices were calculated based on the CRU observation, CHIRPS, and PERSIANN-CDR datasets from 1984 to 2020. The CHIRPS and PERSIANN-CDR estimated rainfall data showed the various meteorological drought events on multiple time scales. These time scales (i.g. 3, 6, 12) describe the short, medium, and long-term drought anomalies that impact water resource availability (Ionita, Scholz, and Chelcea 2016). The temporal evolution of the SPI-3, SPI-6, and SPI-12 indices are depicted in Figure 6 using observed and QPEs satellite products. This figure was generated using mean monthly precipitation datasets. Although, SPI showed satisfactory results in comparison between CRU observation and QPEs datasets. In general, four major drought periods were identified by evaluating the SPI-6 and SPI-12 temporal values over the past 37 years. In SPI-12, the drought events started in 1984 and continued until 2017 at severe drought conditions, but not more significant in the present. However, CHIRPS estimated data gives more accuracy in terms of magnitude and identifies the drought event for all scales.

CHIRPS estimated SPI drought events that started in 1984 were overestimated, and this dry event attenuated in 1994. These results indicate that the SPI values from CHIRPS estimated data were overestimated compared to the CRU observation. Therefore, the drought events estimated from CHIRPS data were more humid (Gao et al. 2018). Although evaluating the SPI-12, CHIRPS identifies the long-lasting and severe drought event (Figure 6(h)), which started approximately 1990 and imprecise during 1995 over the entire period (1984–2020). Similarly, the PERSIANN-CDR estimated SPI-12 showed the highest magnitude of extreme drought event in 1992 (Figure 6(i)), the long drought period estimated by CHIRPS. However, evaluating the performance of capturing the behavior of drought events, CHIRPS showed greater precision than PERSIANN-CDR.

The significant drought event has SPI values less than – 2 and thus was classified as an extreme drought event with high magnitude. Evaluating the behavior of SPI-6, the extreme drought event identified in 1984, 1992, and 1998 for both QPEs estimated data. Figure 6 explains the great magnitude of the drought event, which started in March 1984 and extended until May 2017. Although, PERSIANN-CDR had the highest magnitude (> – 3.0) of extreme drought events compared to CHIRPS (Figure 6(f)). Also, it should be noted that the CHIRPS estimated SPI-6 values have a similar range with referenced CRU observation. Still, most of the PERSIANN-CDR estimated SPI-6 show the overestimated values at extreme dry events. In general, both QPEs estimated SPI-12 described the Similar drought event at a severe scale (>1.5 to – 2) based on the CRU measurement, especially for the 1992 drought event. However, some of the overestimated severe drought found in PERSIANN-CDR estimated data referenced CRU estimated drought event.
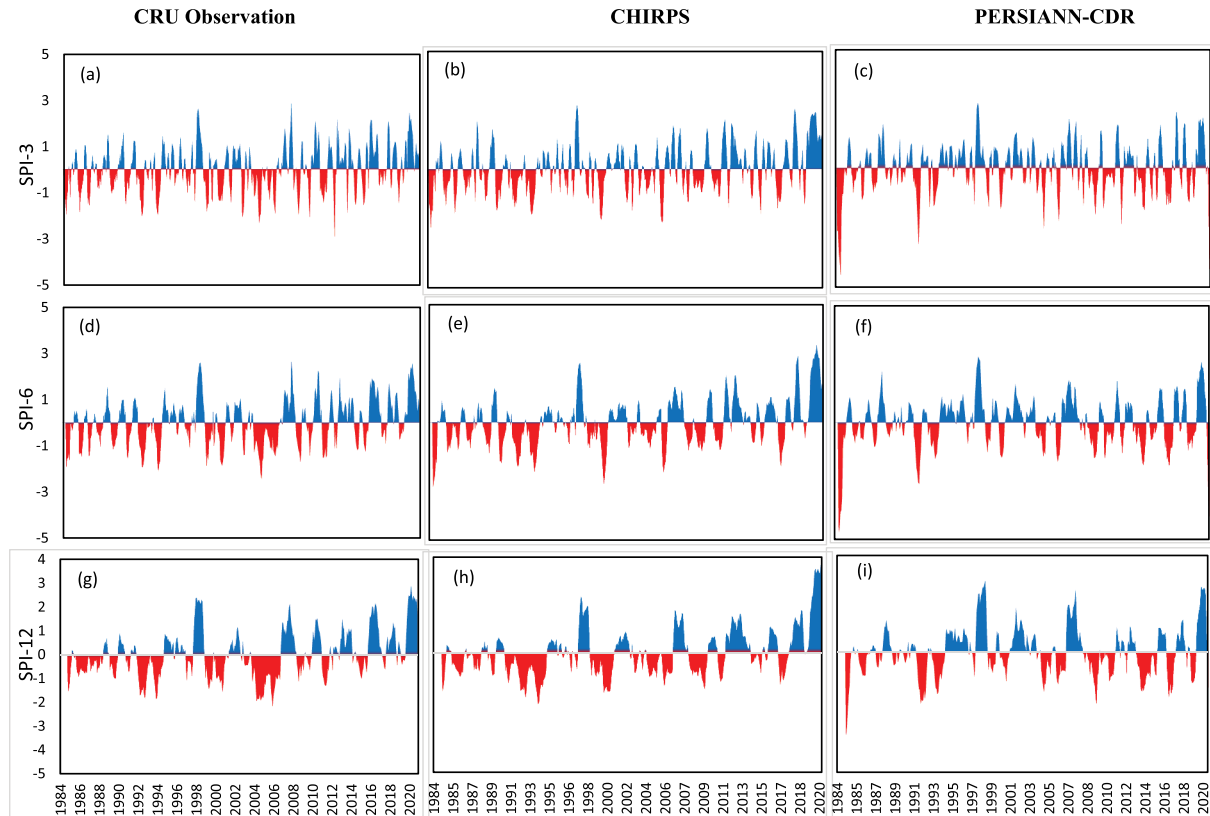
Figure 6. Time-series comparison of averaged SPI-3, SPI-6, and SPI-12 timescale based on CRU observation, CHIRPS and PERSIANN-CDR in 1984–2020. Figures a, d, and g are CRU, figures b, e, and h are CHIRPS and c, f, and I are PERSIANN-CDR.

The output of these studies collaborated with other drought studies, which found similar extreme and severe drought events over the LVB (Awange et al. 2007; Awange 2021). It found that the 1990 to 1995 period is the longest extreme drought event in the analyzed historical period (Awange et al. 2013). Although the strong influence of El-Niño/IOD conditions was recorded from 2006 to 2010 (Evans, Mukhovi, and Nyandega 2020), the long severe drought condition was identified from 2011 to 2015 (Figure 6 (a, b)). It should be noted that the extreme drought event in 1984 affected 200,000 people over LVB (Awange et al. 2007), which increased in the recent drought period (2011–2015). In the present situation, 40 million people living around the LVB are affected by these events and decline the rate of food production. However, no other significant studies indicate the extreme and severe meteorological drought event after 2000. these studies also evaluate the major drought event in the recent past, which is inversely related to the food supply and agriculture production.

Figure 7 shows the scatter plots of SPI (i.e. 3, 6, 12) based on CRU observation, CHIRPS and PERSIANN-CDR estimated precipitation data over the LVB. This visual analysis indicates that most of the PERSIANN-CDR estimated SPI values were overestimated than the values based on CRU observation. On the other hand, the CHIRPS estimated SPI value was less

overestimated and suitable for capturing the drought behavior than the CRU observation. Although, changes influenced the accuracy of estimated SPI values between CRU observation and QPEs products in the multiple time scale. In general, CC, MBE, MAE, and RMSE provide a more accurate assessment of long- and short-term drought. The results indicate the strong correlation agreement between CHIRPS and CRU estimated SPI values with the range of 06–0.72 (Table 4).

In contrast, the PERSIANN-CDR estimated data show low satisfactory results (CC values are less than 0.5) compared to the CRU values. Evaluating the PERSIANN-CDR estimated SPI values show the higher MBE, which exceeds – 0.007 compared to the CHIRPS. Negative MBE values indicate the overestimated values from satellite estimated. However, this error was negligible for assessing the long-term drought monitoring. Also, the same results were identified for MAE when evaluating the SPI values in multiple time scales. The RMSE values indicate the low significant error and do not exceed 0.7 for both the QPEs product. The performance of CHIRPS was better on all the time scale. Therefore, CHIRPS estimated data is more suitable to identify drought events at a multitemporal scale.

Figure 8 shows the temporal comparison of the dry and wet events for SPI-3, SPI-6, and SPI-12 based on the CRU observation, CHIRPS, and PERSIANN-CDR over the LVB. When compared to all of the other
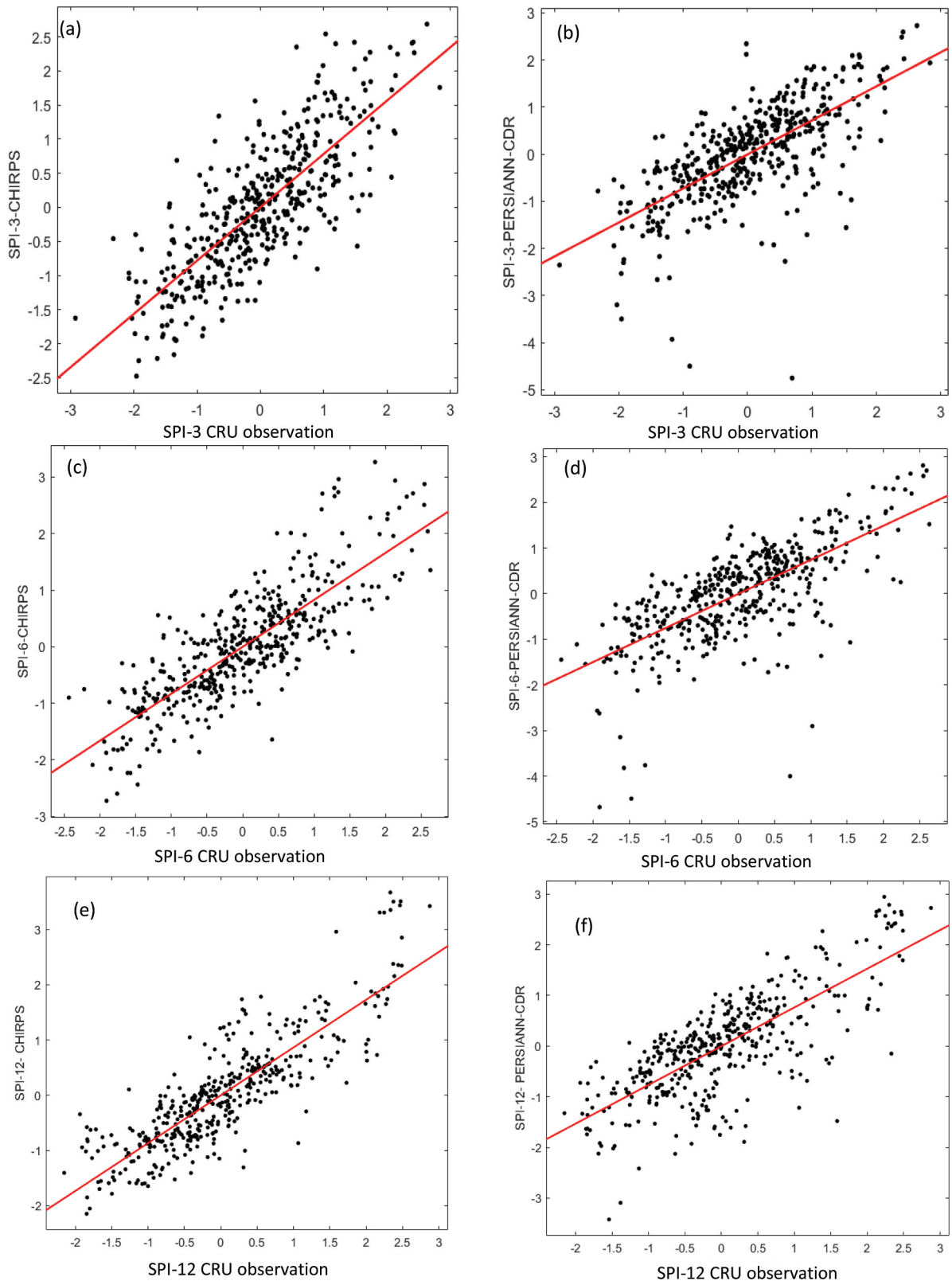
Figure 7. Scatter plot of SPI-3, SPI-6, and SPI-12 based on average monthly precipitation retrieved from CRU observation, CHIRPS, and PERSIANN-CDR estimated data.

events, the percentage of Near Normal conditions was higher. Extreme wet and dry events were less frequent compared to severe and moderate conditions. SPI-3 results show the overestimated frequency for near normal to extremely dry conditions by PERSIANN-CDR. In contrast, CHIRPS data shows a similar frequency percentage for SPI-6 and SPI-12 in dry events.

Comparison between the results of SPI-6 and SPI-12, both the satellite estimated data show the overestimated value for the near-normal event.

In contrast, PERSIANN-CDR indicates more overestimated values for SPI-12 and CHIRPS for SPI-6. Although, the extreme wet event was practically a more significant variation in the SPI-3 than

Table 4. Statistical analysis between CRU observation and QPEs estimated precipitation product based on the SPI indices.

Statistics	CHIRPS			PERSIANN-CDR		
	SPI-3	SPI-6	SPI-12	SPI-3	SPI-6	SPI-12
CC	0.62	0.67	0.72	0.47	0.49	0.57
MBE	0.001	−0.002	−0.001	−0.007	−0.006	−0.001
MAE	0.49	0.47	0.41	0.57	0.56	0.53
RMSE	0.602	0.58	0.52	0.76	0.77	0.657

those in SPI-6. Thus, the events show a similar frequency in the analysis of short and medium-term drought monitoring. In addition, extreme drought event based on CHIRPS estimated data shows a similar frequency to CRU observation. In contrast, PERSIANN-CDR indicates the overestimated results for the three-time scale of SPI (3, 6 and 12). Based on the CHIRPS estimated data, the frequency was similar for all the types of events based on the CRU observation.

3.2.2 Spatial comparison of SPI

Figure 9 depicts the monthly spatial distribution of short, medium, and long-term drought (SPI-3, SPI-6, and SPI-12) events during 2011 and 2012 using CRU observational, CHIRPS, and PERSIANN-CDR estimated data. This period had the highest peak in recent decades from 2010 to 2020, in which 2012 year is more critical than 2011. For short-term drought monitoring, SPI-3 shows the highest peak in February and March under the extreme classification. SPI-12 also recorded the low rainfall and severe drought conditions in October, November, and December. The results indicate a similar spatial distribution for CHIRPS and PERSIANN-CDR estimated data for long-term-drought (SPI-12) events. There is a slight difference between the SPI-12 in February, May, September, and December for CHIRPS, whereas PERSIANN-CDR results are more similar to the CRU observation. For SPI-6, CHIRPS and PERSIANN-CDR presented similar results, which is helpful for medium-range drought monitoring in LVB. Although, PERSIANN-CDR shows the slightly overestimated values for SPI-3 in January and

November. However, CHIRPS estimated spatial distribution shows similar SPI-3, SPI-6, and SPI-12 results based on the CRU observation.

The spatial distribution of extreme drought events in the LVB over multiple time scales from 1984 to 2020 is depicted in Figure 10. The results indicate the high variability among the different QPE products and time scales. It should be noted that the number of the extreme dry event had higher values for the long-term (SPI-12) scale. The spatial distribution between CRU and CHIRPS shows a similar pattern for SPI-6, whereas some underestimated number of dry events were found for SPI-12. But the PERSIANN-CDR estimated results show the overestimated values PERSIANN-CDR data is used. Although, most of the higher number of extreme drought events identify in the Northwestern and southwestern parts of the LVB. For medium and long-term drought monitoring, the number of extreme events increased in the northwestern region.

3.3. Comparison of future drought trend based on Hurst exponent

The R/S analysis was used to estimate the Hurst exponent of SPI values at multiple timescales to predict the drought trend over LVB during 1984–2020. The spatial distribution of the H values of SPI-3, SPI-6 and SPI-12 series of the QPE products was shown in Figure 11. The H value indicates the long memory dependency structure (LTP), ranging from 0 to 1 (Adarsh et al. 2019). According to the H index, the predictability of drought events varies from various scaling ranges of SPI (Millán, Macías, and Rabelo-Lima 2021). For example, the results of the H value from SPI-3 ranged from 0.5 to 0.7, and SPI-6 ranged from 0.55 to 0.77. Whereas for timescale 12, the variation ranges between 0.6 to 0.8. These results indicate that the H exponent degree gradually increases with an increase in timescale (Adarsh et al. 2019). Although, the spatial distribution between CRU observation and CHIRPS shows a similar future drought magnitude for SPI-3 and SPI-6, whereas PERSIANN-CDR product estimated H value shows some overestimated SPI-12.
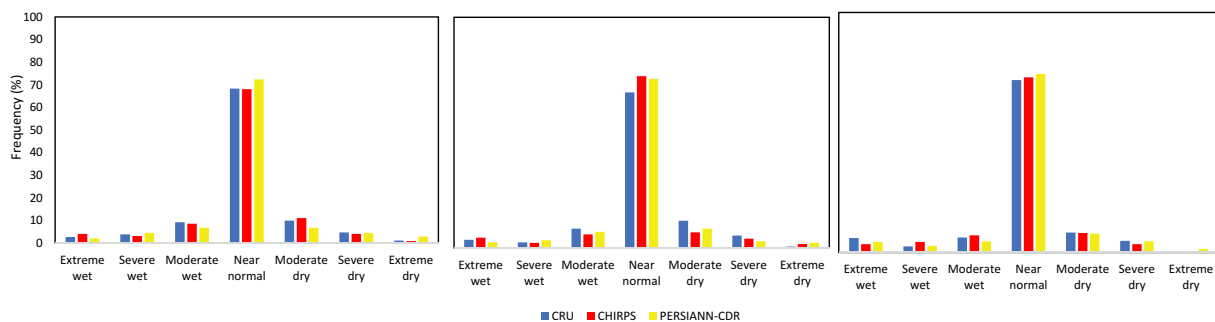
Figure 8. Frequency analysis of dry and wet event categories of SPI at multiple time scales using three different datasets (1984–2020).
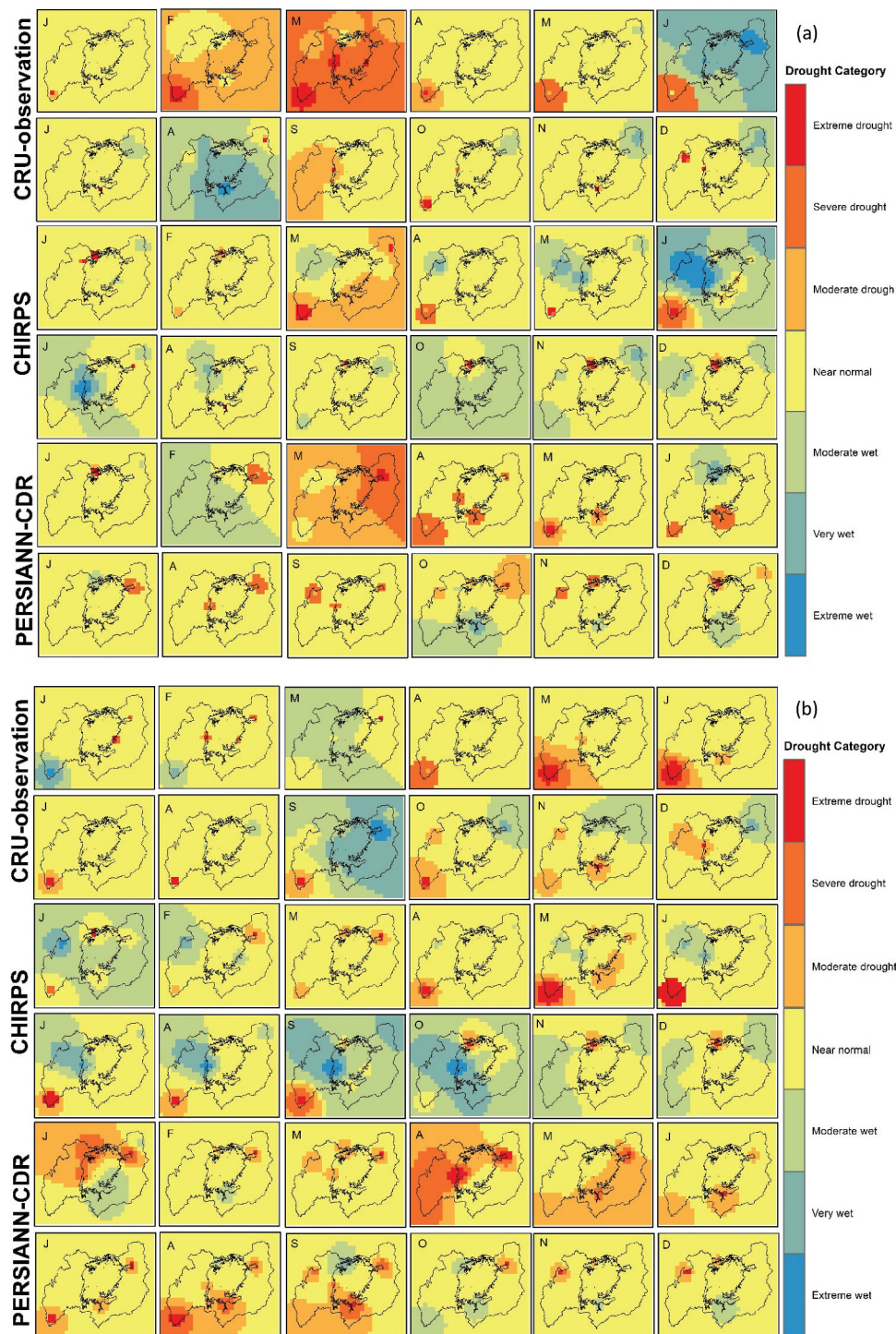
Figure 9. Monthly Spatial distribution of SPI-3 (a), SPI-6 (b) and SPI-12 (c) for 2012 over LVB.

It should be noted that the high H exponent was observed in the north-eastern part of the LVB for both QPE products. The average lowest value of H exponent from CRU observation, CHIRPS and PERSIANN-CDR for SPI-3 (0.56) were recorded in the western part of the LVB. This finding indicates the future drought trend is consistent with the current state in this region. However, the estimated H value from CRU observation and QPE products from all stations in the LVB is higher than 0.5, which indicates the future evolution trend of drought continued to decrease in the future. These reflect that the drought event in LVB is frequent and continuous changes from drier to humid. Moreover, our results have significant implications for strategies to reduce the possibility of damages caused by drought events at different sub-basin levels of LVB.
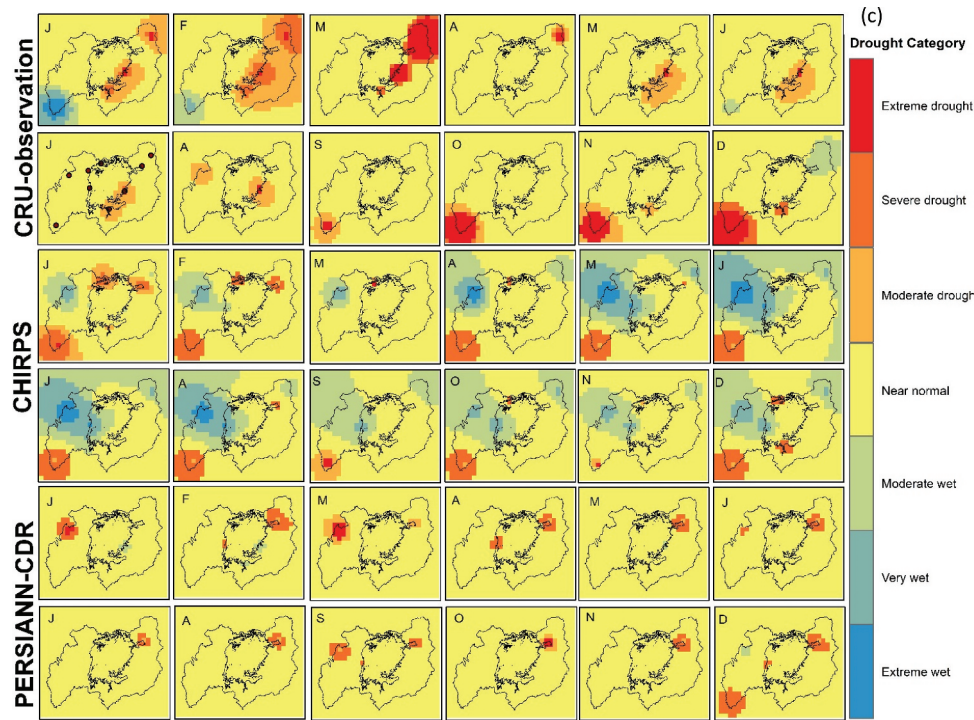
Figure 9. Continued.

4. Discussion

In East Africa, this is the first attempt to evaluate two precipitation products to monitor and predict the trend of drought hazards in the Lake Victoria Basin. In contrast, the community of this region is witnessed the drought event frequently. This study assessed the performance of two widely used QPEs products with long-term data records, such as CHIRPS and PERSIANN-CDR, which indicate an alternative option for station-based observation to detect the drought events. The CRU data has been taken as reference data for comparison. These studies promote satellite precipitation products to monitor climatic events, natural hazards, and other relevant studies. In general, these two QPE products performed well to detect the drought events in the eastern and south-western parts of LVB. Although CHIRPS present better performance for several regions of LVB, also PERSIANN-CDR performed satisfactory results to detect this drought hazard in the studied region. Thus, both CHIRPS and PERSIANN-CDR can monitor and predict the drought events on the local scale and be used in the different semi-arid regions (Bouaziz, Medhioub, and Csaplovisc 2021; de Brito et al. 2021). In comparing CHIRPS data, PERSIANN-CDR is relatively weak for relevant the drought events spatial pattern due to coarse spatial resolution (0.25°) and corrected by GPCP data (Zhong et al. 2019). Therefore, awareness should be taken while studying the spatial characteristics of drought events using PERSIANN-CDR. At the same time, CHIRPS data have a high spatial resolution (0.05°) and are corrected by the in-situ gauge observation (Pandey et al. 2020). As per the results,

CHIRPS performance is superior to PERSIANN-CDR for monitoring and predicting the drought events over LVB and validated by other studies (Shrestha et al. 2017; Gao et al. 2018; Lai et al. 2019).

Zhao and Ma (2019) compared four QPEs products such as TRMM, CHIRPS, CMORPH-BLD and PERSIANN- CDR for meteorological drought monitoring in a global scale evaluation. This study found that the CHIRPS performed well for Africa, whereas PERSIANN-CDR has satisfactory performance for this region (except Central Africa). In addition, Atiah et al. (2020) evaluated various satellite precipitation products and observed that the CHIRPS had better skill over Ghana, West Africa. These all findings are similar to our findings and reveal the importance of QPEs products. For example, PBIAS and MKGE score distribution indicate excellent performance for CHIRPS products over the LVB. In some cases, PBIAS and MKGE scores are still low for some western parts of the LVB, due to the poor accuracy of QPEs products. Therefore, these regions are unsuitable for evaluating the QPEs product for drought monitoring. Further evaluation is important using a local gauge network for correcting the QPEs products. However, sparse gauge networks limit the evaluation of QPEs studies over Africa.

This study used the Hurst exponent to estimate the future drought trend over the LVB and compared it with these two QPEs products. As per the results, both QPEs products show good agreement to predict the future drought trend. Since the H values from QPEs and CRU observation are higher than 0.5, which indicate, the future drought trend will be decreased. However, CHIRPS performed well compared to
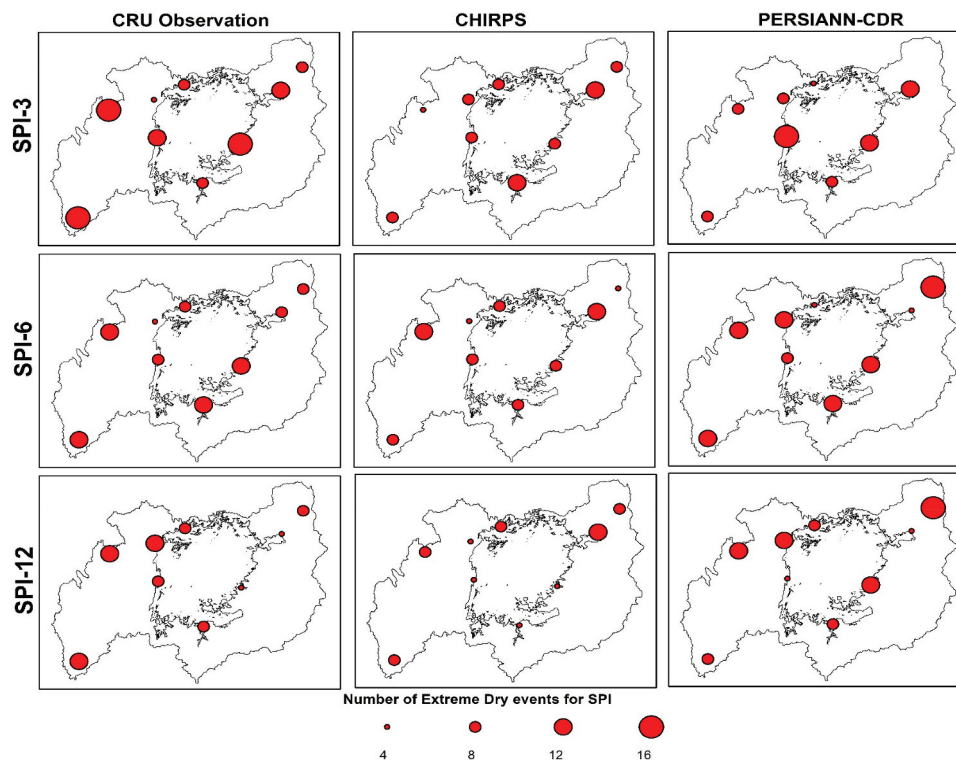
Figure 10. Spatial distribution of the number of extreme dry events considering SPI-3, SPI-6, and SPI-12 over the LVB (1984–2020).
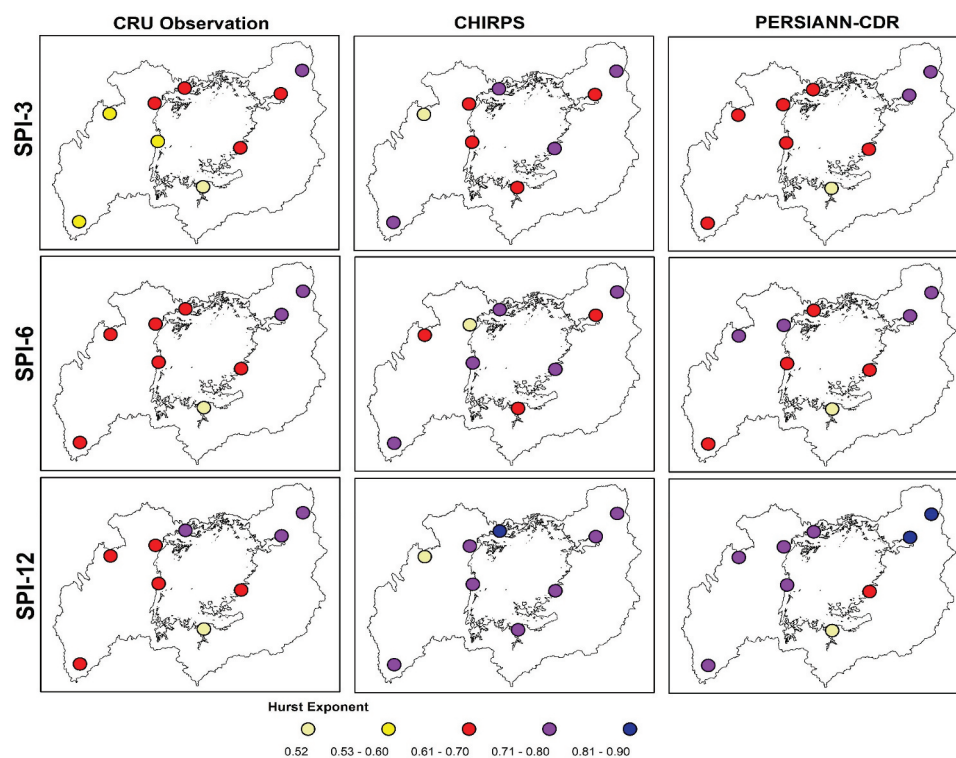

Figure 11. Spatial distribution of the Hurst Exponent (H) considering SPI-3, SPI-6, and SPI-12 over the LVB (1984–2020).

PERSIANN-CDR for capturing the future drought trend over LVB. Therefore, it is suggested that the CHIRPS data can be used as an alternative option for rain-gauge observation to predict the future drought trend. Although, this analysis cannot forecast the length of the predicted drought trend in the future and cannot predict future drought events in various categories (Tong et al. 2018). This present study also recommended that the H exponent be useful in developing water management policies over LVB (Tatli 2015).

5. Conclusion

Long-term satellite-based QPEs provide an optional precipitation source for meteorological drought monitoring. This study evaluates more than 37 years of QPEs precipitation datasets (CHIRPS and PERSIANN-CDR) for monitoring the meteorological drought indices over the Lake Victoria Basin. The spatial and temporal patterns of drought conditions were identified based on SPI-3, SPI-6, and SPI-12. The highest rainfall pattern was found at greater than 200 mm per year from 2018 to 2020. The year with below-average rainfall anomaly over the LVB was 1984, 1990, 1992, 1993, 1995, 2003, 2004 and 2005, and 1990 to 1995, recorded for the most extended period low rainfall. SPI-3, SPI-6, and SPI-12 results show the major drought event in the recent decade in the LVB. CHIRPS datasets found the main drought events with some underestimated and overestimation values which is negligible. PERSIANN-CDR captures the drought event but is more overestimated for SPI values. The results of PERSIANN-CDR presented poorer but still acceptable with negative MBE (−0.006) and RMSE of 0.7 for both calibration and validation. This study also examined the future drought trend over LVB using the H exponent and predicted that the degree of drought trend would decrease in the future. Also, the predicted results from CHIRPS are closed to observation, and this product is recommended as an alternative option for station-based observation. The outcome of this study highlighted capturing the drought event in the recent decade and future drought trends and providing information for policymakers to reduce the social and economic impact, especially agriculture and water supply. However, the production of CHIRPS data takes a long time for error correction using in-situ observation; therefore, it is unsuitable for "strict-real-time" applications. In addition, PERSIANN-CDR is only suitable for historical drought assessment due to their long lag time. Moreover, drought is a long-term climate phenomenon compared to floods and needs a larger timescale. For this reason, these two QPEs products are acceptable for "near-real-time" drought assessment. Therefore, real-time and near-real-time QPEs were needed to develop with a higher timescale for drought monitoring using short-term and long term QPEs.

Data availability statement

Publicly available datasets were analysed in this study. This data can be found here: https://sites.uea.ac.uk/cru/data, https://www.chc.ucsb.edu/data/chirps and https://chrsdata.eng.uci.edu/. Also, Derived data supporting the finding of this study are available from the corresponding author on request.

Ethical Approval

All the work complies with Ethical standards

Consent of Participate

Not applicable

Disclosure statement

No potential conflict of interest was reported by the author(s).

Notes on contributors

Priyanko Das is a research fellow in the Institute of African Studies, School of Geography and Oceanography sciences, Nanjing University. His research interest includes African Climate change, glacier studies, Hydrology, Environment, and Remote sensing. His research works have been published in peer-reviewed journals and received various awards from different organizations.

Zhenke Zhang is a professor in the school of geography and ocean science, Nanjing University. He is the secretary-general of China Society for African Studies, also is the director of the Institute of African Studies at Nanjing University. His current research interests are African coastal resources and environment, African economic geography, and marine economy.

Hang Ren is a research assistant professor of Institute of Population Studies, Nanjing University of Post and Telecommunication. He received his Ph.D. from Institute of African Studies, school of geography and ocean science, Nanjing University with major in Human Geography. His research interest includes African geography, Urban Population Studies and Sustainable Development.

References

Abrha, H., and H. Hagos. 2019. "Future Drought and Aridity Monitoring Using Multi-model Approach under Climate Change in Hintalo Wejerat District, Ethiopia." *Sustainable Water Resources Management* 5 (4): 1963–1972. doi:10.1007/s40899-019-00350-1.

Adarsh, S., D.N. Kumar, B. Deepthi, G. Gayathri, S.S. Aswathy, and S. Bhagyasree. 2019. "Multifractal Characterization of Meteorological Drought in India Using Detrended Fluctuation Analysis." *International Journal of Climatology* 39 (11): 4234–4255. doi:10.1002/joc.6070.

Anyah, R.O., F.H.M. Semazzi, and L. Xie. 2006. "Simulated Physical Mechanisms Associated with Climate Variability over Lake Victoria Basin in East Africa." *Monthly Weather Review* 134 (12): 3588–3609. doi:10.1175/MWR3266.1.

Arheimer, B. 2021. "Landscape Perspectives in Hydrological Understanding and Modelling for Water Management." *European Geosciences Union*, Online meeting, Apirl 19-30. doi: 10.5194/egusphere-egu21-12778.

Atiah, W.A., L.K. Amekudzi, J.N.A. Aryee, K. Preko, and S. K. Danuor. 2020. "Validation of Satellite and Merged Rainfall Data over Ghana, West Africa." *Atmosphere* 11 (8): 859. doi:10.3390/atmos11080859.

Awange, J. 2021. *Lake Victoria Monitored from Space*. Cham: Springer International Publishing.

Awange, J., J. Aluoch, L. Ogallo, M. Omulo, and P. Omondi. 2007. "Frequency and Severity of Drought in the Lake Victoria Region (Kenya) and Its Effects on Food Security." *Climate Research* 33: 135–142. doi:10.3354/cr033135.

Awange, J.L., R. Anyah, N. Agola, E. Forootan, and P. Omondi. 2013. "Potential Impacts of Climate and Environmental Change on the Stored Water of Lake Victoria Basin and Economic Implications: Impacts of Climate Change on Waters of Lake Victoria." *Water Resources Research* 49 (12): 8160–8173. doi:10.1002/2013WR014350.

Bouaziz, M., E. Medhioub, and E. Csaplovisc. 2021. "A Machine Learning Model for Drought Tracking and Forecasting Using Remote Precipitation Data and A Standardized Precipitation Index from Arid Regions." *Journal of Arid Environments* 189: 104478. doi:10.1016/j.jaridenv.2021.104478.

Chen, C., Z. Li, Y. Song, Z. Duan, K. Mo, Z. Wang, and Q. Chen. 2020. "Performance of Multiple Satellite Precipitation Estimates over a Typical Arid Mountainous Area of China: Spatiotemporal Patterns and Extremes." *Journal of Hydrometeorology* 21 (3): 533–550. doi:10.1175/JHM-D-19-0167.1.

Danandeh Mehr, A., A.U. Sorman, E. Kahya, and M.H. Afshar. 2020. "Climate Change Impacts on Meteorological Drought Using SPI and SPEI: Case Study of Ankara, Turkey." *Hydrological Sciences Journal* 65 (2): 254–268. doi:10.1080/02626667.2019.1691218.

de Brito, C.S., R.M. da Silva, C.A.G. Santos, R.M.B. Neto, and V.H.R. Coelho. 2021. "Monitoring Meteorological Drought in A Semiarid Region Using Two Long-term Satellite-estimated Rainfall Datasets: A Case Study of the Piranhas River Basin, Northeastern Brazil." *Atmospheric Research* 250: 105380. doi:10.1016/j.atmosres.2020.105380.

Dehghan, S., N. Salehnia, N. Sayari, and B. Bakhtiari. 2020. "Prediction of Meteorological Drought in Arid and Semi-arid Regions Using PDSI and SDSM: A Case Study in Fars Province, Iran." *Journal of Arid Land* 12 (2): 318–330. doi:10.1007/s40333-020-0095-5.

Dikici, M. 2020. "Drought Analysis with Different Indices for the Asi Basin (Turkey)." *Scientific Reports* 10 (1): 20739. doi:10.1038/s41598-020-77827-z.

Evans, W.O., S.N. Mukhovi, and I.A. Nyandega. 2020. "The Spatial and Temporal Characteristics of Rainfall over the Lake Victoria Basin of Kenya in 1987-2016." *Atmospheric and Climate Sciences* 10 (2): 240–257. doi:10.4236/acs.2020.102013.

Feng, W., H. Lu, T. Yao, and Q. Yu. 2020. "Drought Characteristics and Its Elevation Dependence in the Qinghai–Tibet Plateau during the Last Half-century." *Scientific Reports* 10 (1): 14323. doi:10.1038/s41598-020-71295-1.

Gao, F., Y. Zhang, X. Ren, Y. Yao, Z. Hao, and W. Cai. 2018. "Evaluation of CHIRPS and Its Application for Drought Monitoring over the Haihe River Basin, China." *Natural Hazards* 92 (1): 155–172. doi:10.1007/s11069-018-3196-0.

Ghozat, A., A. Sharafati, and S.A. Hosseini. 2021. "Long-term Spatiotemporal Evaluation of CHIRPS Satellite Precipitation Product over Different Climatic Regions of Iran." *Theoretical and Applied Climatology* 143 (1–2): 211–225. doi:10.1007/s00704-020-03428-5.

Guo, H., A. Bao, T. Liu, S. Chen, and F. Ndayisaba. 2016. "Evaluation of PERSIANN-CDR for Meteorological Drought Monitoring over China." *Remote Sensing* 8 (5): 379. doi:10.3390/rs8050379.

Harris, I., T.J. Osborn, P. Jones, and D. Lister. 2020. "Version 4 of the CRU TS Monthly High-resolution Gridded Multivariate Climate Dataset." *Scientific Data* 7 (1): 109. doi:10.1038/s41597-020-0453-3.

Hayes, M., M. Svoboda, N. Wall, and M. Widhalm. 2011. "The Lincoln Declaration on Drought Indices: Universal Meteorological Drought Index Recommended." *Bulletin of the American Meteorological Society* 92 (4): 485–488. doi:10.1175/2010BAMS3103.1.

Huang, S., Q. Huang, G. Leng, and J. Chang. 2016. "A Hybrid Index for Characterizing Drought Based on A Nonparametric Kernel Estimator." *Journal of Applied Meteorology and Climatology* 55 (6): 1377–1389. doi:10.1175/JAMC-D-15-0295.1.

Huang, B., and J. Wang. 2020. "Big Spatial Data for Urban and Environmental Sustainability." *Geo-Spatial Information Science* 23 (2): 125–140. doi:10.1080/10095020.2020.1754138.

Hurst, H.E. 1951. "Long-Term Storage Capacity of Reservoirs." *Transactions of the American Society of Civil Engineers* 116 (2). doi:10.1061/TACEAT.0006518.

Ionita, M., P. Scholz, and S. Chelcea. 2016. "Assessment of Droughts in Romania Using the Standardized Precipitation Index." *Natural Hazards* 81 (3): 1483–1498. doi:10.1007/s11069-015-2141-8.

Kassaye, A.Y., G. Shao, X. Wang, and S. Wu. 2021. "Quantification of Drought Severity Change in Ethiopia during 1952–2017." *Environment, Development and Sustainability* 23 (4): 5096–5121. doi:10.1007/s10668-020-00805-y.

Kizza, M., A. Rodhe, C.Y. Xu, H.K. Ntale, and S. Halldin. 2009. "Temporal Rainfall Variability in the Lake Victoria Basin in East Africa during the Twentieth Century." *Theoretical and Applied Climatology* 98 (1–2): 119–135. doi:10.1007/s00704-008-0093-6.

Kizza, M., I. Westerberg, A. Rodhe, and H.K. Ntale. 2012. "Estimating Areal Rainfall over Lake Victoria and Its Basin Using Ground-based and Satellite Data." *Journal of Hydrology* 464–465: 401–411. doi:10.1016/j.jhydrol.2012.07.024.

Kling, H., M. Fuchs, and M. Paulin. 2012. "Runoff Conditions in the Upper Danube Basin under an Ensemble of Climate Change Scenarios." *Journal of Hydrology* 424: 264–277. doi:10.1016/j.jhydrol.2012.01.011.

Kubicz, J. 2018. "The Application of Standardized Precipitation Index (SPI) to Monitor Drought in Surface and Groundwaters." *E3S Web of Conferences*, Wroclaw, July 2-5. doi:10.1051/e3sconf/20184400082.

Lai, C., R. Zhong, Z. Wang, X. Wu, X. Chen, P. Wang, and Y. Lian. 2019. "Monitoring Hydrological Drought Using Long-term Satellite-based Precipitation Data." *Science of the Total Environment* 649: 1198–1208. doi:10.1016/j.scitotenv.2018.08.245.

Liu, C., C. Yang, Q. Yang, and J. Wang. 2021. "Spatiotemporal Drought Analysis by the Standardized Precipitation Index (SPI) and Standardized Precipitation Evapotranspiration Index (SPEI) in Sichuan Province, China." *Scientific Reports* 11 (1): 1280. doi:10.1038/s41598-020-80527-3.

Malik, A., A. Kumar, O. Kisi, N. Khan, S.Q. Salih, and Z.M. Yaseen. 2021. "Analysis of Dry and Wet Climate Characteristics at Uttarakhand (India) Using Effective Drought Index." *Natural Hazards* 105 (2): 1643–1662. doi:10.1007/s11069-020-04370-5.

Mandelbrot, B.B., and J.R. Wallis. 1969. "Robustness of the Rescaled Range R/S in the Measurement of Noncyclic Long Run Statistical Dependence." *Water Resources Research* 5 (5): 967–988. doi:10.1029/WR005i005p00967.

McKee, T.B., N.J. Doesken, and J. Kleist. 1993. "The Relationship Of Drought Frequency And Duration To Time Scales." *the 8th Conference on Applied Climatology*, Anaheim, January 17-22.

Millán, H., I. Macías, and J. Rabelo-Lima. 2021. "Hurst Scaling with Crossover of A Drought Indicator: A Case Study in Belem and Manaus, Brazil." *Natural Hazards*. doi:10.1007/s11069-021-04937-w.

Mohseni, F., M.K. Sadr, S. Eslamian, A. Areffian, and A. Khoshfetrat. 2021. "Spatial and Temporal Monitoring of Drought Conditions Using the Satellite Rainfall Estimates and Remote Sensing Optical and Thermal Measurements." *Advances in Space Research* 67 (12): 3942–3959. doi:10.1016/j.asr.2021.02.017.

Mugo, R., R. Waswa, J.W. Nyaga, A. Ndubi, E.C. Adams, and A.I. Flores-Anderson. 2020. "Quantifying Land Use Land Cover Changes in the Lake Victoria Basin Using Satellite Remote Sensing: The Trends and Drivers between 1985 and 2014." *Remote Sensing* 12 (17): 2829. doi:10.3390/rs12172829.

Musonda, B., Y. Jing, V. Iyakaremye, and M. Ojara. 2020. "Analysis of Long-Term Variations of Drought Characteristics Using Standardized Precipitation Index over Zambia." *Atmosphere* 11 (12): 1268. doi:10.3390/atmos11121268.

Mutti, P.R., V. Dubreuil, B.G. Bezerra, D. Arvor, C.P. de Oliveira, and C.M. Santos E Silva. 2020. "Assessment of Gridded CRU TS Data for Long-Term Climatic Water Balance Monitoring over the São Francisco Watershed, Brazil." *Atmosphere* 11 (11): 1207. doi:10.3390/atmos11111207.

Nguyen, P., E.J. Shearer, H. Tran, M. Ombadi, N. Hayatbini, T. Palacios, P. Huynh, et al. 2019. "The CHRS Data Portal, an Easily Accessible Public Repository for PERSIANN Global Satellite Precipitation Data." *Scientific Data* 6 (1): 180296. doi:10.1038/sdata.2018.296.

Noorisameleh, Z., W.A. Gough, and M.M.Q. Mirza. 2021. "1951–1959: Evaluation of Drought Severity Changes in Iran Using Hurst Exponent and Standardized Precipitation Index." In *Recent Advances in Environmental Science from the Euro-Mediterranean and Surrounding Regions. 2nd Edition)* ed. 1951–1959. Cham: Springer International Publishing.

Odada, E.O., D.O. Olago, F. Bugenyi, K. Kulindwa, J. Karimumuryango, K. West, M. Ntiba, S. Wandiga, P. Aloo-Obudho, and P. Achola. 2003. "Environmental Assessment of the East African Rift Valley Lakes." *Aquatic Sciences - Research Across Boundaries* 65 (3): 254–271. doi:10.1007/s00027-003-0638-9.

Oliver, R., and J.L. Ballester. 1996. "Rescaled Range Analysis of the Asymmetry of Solar Activity." *Solar Physics* 169 (1): 215–224. doi:10.1007/BF00153842.

Pandey, V., P.K. Srivastava, R.K. Mall, F. Munoz-Arriola, and D. Han. 2020. "Multi-satellite Precipitation Products for Meteorological Drought Assessment and Forecasting in Central India." *Geocarto International* 1–20. doi:10.1080/10106049.2020.1801862.

Pathak, A.A., and B.M. Dodamani. 2020. "Comparison of Meteorological Drought Indices for Different Climatic Regions of an Indian River Basin." *Asia-Pacific Journal of Atmospheric Sciences* 56 (4): 563–576. doi:10.1007/s13143-019-00162-5.

Phoon, S.Y., A.Y. Shamseldin, and K. Vairavamoorthy. 2004. "Assessing Impacts of Climate Change on Lake Victoria Basin, Africa." *the 30th WEDC International Conference*, Vientiane, October 25-29.

Rahman, K.U., S. Shang, M. Shahid, and Y. Wen. 2019. "Performance Assessment of SM2RAIN-CCI and SM2RAIN-ASCAT Precipitation Products over Pakistan." *Remote Sensing* 11 (17): 2040. doi:10.3390/rs11172040.

Rahman, K.U., S. Shang, M. Shahid, Y. Wen, and A.J. Khan. 2020. "Development of a Novel Weighted Average Least Squares-based Ensemble Multi-satellite Precipitation Dataset and Its Comprehensive Evaluation over Pakistan." *Atmospheric Research* 246: 105133. doi:10.1016/j.atmosres.2020.105133.

Saeedi, M., A. Sharafati, and A. Tavakol. 2021. "Evaluation of Gridded Soil Moisture Products over Varied Land Covers, Climates, and Soil Textures Using in Situ Measurements: A Case Study of Lake Urmia Basin." *Theoretical and Applied Climatology* 145 (3–4): 1053–1074. doi:10.1007/s00704-021-03678-x.

Salehnia, N., A. Alizadeh, H. Sanaeinejad, M. Bannayan, A. Zarrin, and G. Hoogenboom. 2017. "Estimation of Meteorological Drought Indices Based on AgMERRA Precipitation Data and Station-observed Precipitation Data." *Journal of Arid Land* 9 (6): 797–809. doi:10.1007/s40333-017-0070-y.

Salmani-Dehaghi, N., and N. Samani. 2019. "Spatiotemporal Assessment of the PERSIANN Family of Satellite Precipitation Data over Fars Province, Iran." *Theoretical and Applied Climatology* 138 (3–4): 1333–1357. doi:10.1007/s00704-019-02872-2.

Santos, C.A.G., R.M.B. Neto, T.V.M. Nascimento, R.M. da Silva, M. Mishra, and T.G. Frade. 2021. "Geospatial Drought Severity Analysis Based on PERSIANN-CDR-estimated Rainfall Data for Odisha State in India (1983–2018)." *Science of the Total Environment* 750: 141258. doi:10.1016/j.scitotenv.2020.141258.

Shahid, M., and K.U. Rahman. 2021. "Identifying the Annual and Seasonal Trends of Hydrological and Climatic Variables in the Indus Basin Pakistan." *Asia-Pacific Journal of Atmospheric Sciences* 57 (2): 191–205. doi:10.1007/s13143-020-00194-2.

Shahid, M., K.U. Rahman, S. Haider, H.F. Gabriel, A.J. Khan, Q. B. Pham, B. Mohammadi, N.T.T. Linh, and D.T. Anh. 2021. "Assessing the Potential and Hydrological Usefulness of the CHIRPS Precipitation Dataset over a Complex Topography in Pakistan." *Hydrological Sciences Journal* 66 (11): 1664–1684. doi:10.1080/02626667.2021.1957476.

Shao, Z., N.S. Sumari, A. Portnov, F. Ujoh, W. Musakwa, and P.J. Mandela. 2021. "Urban Sprawl and Its Impact on Sustainable Urban Development: A Combination of Remote Sensing and Social Media Data." *Geo-Spatial Information Science* 24 (2): 241–255. doi:10.1080/10095020.2020.1787800.

Shobeiri, S., A. Sharafati, and A. Neshat. 2021. "Evaluation of Different Gridded Precipitation Products in Trend Analysis of Precipitation Features over Iran." *Acta Geophysica* 69 (3): 959–974. doi:10.1007/s11600-021-00595-5.

Shrestha, N.K., F.M. Qamer, D. Pedreros, M.S.R. Murthy, S. M. Wahid, and M. Shrestha. 2017. "Evaluating the Accuracy of Climate Hazard Group (CHG) Satellite Rainfall Estimates for Precipitation-based Drought Monitoring in Koshi Basin, Nepal." *Journal of Hydrology: Regional Studies* 13: 138–151. doi:10.1016/j.ejrh.2017.08.004.

Svoboda, M., M. Hayes, and D. Wood. 2012. "Standardized Precipitation Index User Guide." *World Meteorological Organization (WMO)-No.* 1090, 16, Geneva. 97892631 10916. 9789263110916.

Tatli, H. 2015. "Detecting Persistence of Meteorological Drought *via* the Hurst Exponent: Persistence of Meteorological Drought *via* Hurst Exponent." *Meteorological Applications* 22 (4): 763–769. doi:10.1002/met.1519.

Tigkas, D., H. Vangelis, and G. Tsakiris. 2019. "Drought Characterisation Based on an Agriculture-oriented Standardised Precipitation Index." *Theoretical and Applied Climatology* 135 (3–4): 1435–1447. doi:10.1007/s00704-018-2451-3.

Tong, S., Q. Lai, J. Zhang, Y. Bao, A. Lusi, Q. Ma, X. Li, and F. Zhang. 2018. "Spatiotemporal Drought Variability on the Mongolian Plateau from 1980–2014 Based on the SPEI-PM, Intensity Analysis and Hurst Exponent." *Science of the Total Environment* 615: 1557–1565. doi:10.1016/j.scitotenv.2017.09.121.

Trinder, J., and Q. Liu. 2020. "Assessing Environmental Impacts of Urban Growth Using Remote Sensing." *Geo-Spatial Information Science* 23 (1): 20–39. doi:10.1080/10095020.2019.1710438.

van der Schrier, G., J. Barichivich, K.R. Briffa, and P.D. Jones. 2013. "A scPDSI-based Global Data Set of Dry and Wet Spells for 1901-2009: Variations in the Self-Calibrating PDSI." *Journal of Geophysical Research: Atmospheres* 118 (10): 4025–4048. doi:10.1002/jgrd.50355.

Wei, W., J. Zhang, J. Zhou, L. Zhou, B. Xie, and C. Li. 2021. "Monitoring Drought Dynamics in China Using Optimized Meteorological Drought Index (OMDI) Based on Remote Sensing Data Sets." *Journal of Environmental Management* 292: 112733. doi:10.1016/j.jenvman.2021.112733.

Yaseen, Z.M., M. Ali, A. Sharafati, N. Al-Ansari, and S. Shahid. 2021. "Forecasting Standardized Precipitation Index Using Data Intelligence Models: Regional Investigation of Bangladesh." *Scientific Reports* 11 (1): 3435. doi:10.1038/s41598-021-82977-9.

Yin, X., and S.E. Nicholson. 1998. "The Water Balance of Lake Victoria." *Hydrological Sciences Journal* 43 (5): 789–811. doi:10.1080/02626669809492173.

Zhang, H., J. Song, G. Wang, X. Wu, and J. Li. 2021. "Spatiotemporal Characteristic and Forecast of Drought in Northern Xinjiang, China." *Ecological Indicators* 127: 107712. doi:10.1016/j.ecolind.2021.107712.

Zhao, H., and Y. Ma. 2019. "Evaluating the Drought-Monitoring Utility of Four Satellite-Based Quantitative Precipitation Estimation Products at Global Scale." *Remote Sensing* 11 (17): 2010. doi:10.3390/rs11172010.

Zhong, R., X. Chen, C. Lai, Z. Wang, Y. Lian, H. Yu, and X. Wu. 2019. "Drought Monitoring Utility of Satellite-based Precipitation Products across Mainland China." *Journal of Hydrology* 568: 343–359. doi:10.1016/j.jhydrol.2018.10.072.

Zhu, S., Z. Ma, J. Xu, K. He, H. Liu, Q. Ji, G. Tang, H. Hu, and H. Gao. 2021. "A Morphology-Based Adaptively Spatio-Temporal Merging Algorithm for Optimally Combining Multisource Gridded Precipitation Products with Various Resolutions." *IEEE Transactions on Geoscience and Remote Sensing* 1–21. doi:10.1109/TGRS.2021.3097336.